

Quantum repeaters based on Rydberg-blockade coupled atomic ensembles

Yang Han^{1,2}, Bing He¹, Khabat Heshami¹, Cheng-Zu Li², and Christoph Simon¹

¹ *Institute for Quantum Information Science and Department of Physics and Astronomy,
University of Calgary, Calgary T2N 1N4, Alberta, Canada*

² *College of Science, National University of Defense Technology, Changsha 410073, China.*

(Dated: November 5, 2018)

We propose a scheme for realizing quantum repeaters with Rydberg-blockade coupled atomic ensembles, based on a recently proposed collective encoding strategy. Rydberg-blockade mediated two-qubit gates and efficient cooperative photon emission are employed to create ensemble-photon entanglement. Thanks to deterministic entanglement swapping operations via Rydberg-based two-qubit gates, and to the suppression of multi-excitation errors by the blockade effect, the entanglement distribution rate of the present scheme is higher by orders of magnitude than the rates achieved by other ensemble-based repeaters. We also show how to realize temporal multiplexing with this system, which offers an additional speedup in entanglement distribution.

PACS numbers: 03.67.Hk, 32.80.Ee, 42.50.Ex

I. INTRODUCTION

Quantum communication aims at secure message transmission between remote locations by employing entanglement for quantum teleportation [1] or quantum cryptography [2]. Unfortunately, since the inevitable photon loss scales exponentially with the length of channel, it is difficult to establish high quality entanglement over long distances. This problem may be overcome by quantum repeaters [3], which create and store shorter-distance entanglement in a heralded way, and then connect the elementary entangled states to establish longer-distance entanglement via entanglement swapping.

A highly influential protocol for realizing quantum repeaters was proposed by Duan, Lukin, Cirac and Zoller (DLCZ)[4]. It is based on macroscopic atomic ensemble quantum memories, Raman scattering and linear optics. There is a significant body of theoretical [5–8] and experimental [9] work based on this general approach. In this paper, we refer to these schemes as DLCZ-type repeaters. The significant advantage of DLCZ-type repeaters is that they use relatively simple elements. However, there are two intrinsic limitations in this approach. First, as Raman scattering is used to create entanglement between a single atomic excitation and a single photon, inevitable multi-excitation (and multi-photon) terms cause errors in the final states. In order to suppress multiple excitations, one has to work with very low excitation probability [4]. Second, the Bell measurements in the swapping operations are realized via linear optics, so the success probability of the entanglement swapping is bounded by $1/2$ [10]. The above two limitations significantly diminish the efficiency of DLCZ-type repeaters.

There are a number of proposals for realizing quantum repeaters using ingredients other than atomic ensembles and linear optics [11–13]. Most of them use individual quantum systems as the quantum memory [12, 13]. An obvious advantage of using individual quantum systems is that the problem of multiple excitations is eliminated. If the two-qubit gates for Bell measurement in the swapping operations can also be realized efficiently, repeaters based on individual quantum systems have the potential to significantly outperform DLCZ-type repeaters [12, 13]. However, for the individual quantum

systems one has to precisely address every single particle, and one may need cavities to achieve a high efficiency of photon collection [13].

An attractive technique for quantum information processing (QIP) with atomic ensembles is based on the Rydberg blockade mechanism, cf. below. There have been a number of proposals to use the Rydberg blockade for various QIP tasks (see [14] for an overview). In the present paper, we propose a concrete scheme for realizing quantum repeaters in this way and analyze its performance in detail. We show that the entanglement distribution rate offered by repeaters based on Rydberg blockade coupled ensembles significantly surpasses the rate of DLCZ-type repeaters. Compared to the schemes involving individual quantum systems, repeaters based on Rydberg blockade coupled ensembles achieve almost the same distribution rate and avoid addressing single particles and using cavities. Our proposed scheme also allows temporal multiplexing [15], which could further enhance the achievable distribution rate.

II. RYDBERG BLOCKADE COUPLED ATOMIC ENSEMBLE

Rydberg states are states of alkali atoms characterized by a high principal quantum number. Atoms in such Rydberg states have large size and can therefore have large dipole moments, resulting in strong dipole-dipole interactions [16]. Due to this strong long-range interaction, a single atom in an atomic ensemble excited to a Rydberg state shifts the Rydberg energy level of its neighbors out of resonance and blocks further excitations, which is called the Rydberg blockade mechanism [17], and this kind of ensembles is referred to as Rydberg blockade coupled ensembles [14]. Recently, experiments have demonstrated an almost perfect blockade [18] as well as a blockade-based C-NOT gate [19] between a single pair of trapped atoms at separation $R \leq 10\mu\text{m}$. Although no experiments have been done with an ensemble where the blockade acts across the whole ensemble, a number of experiments show clear signs of the blockade effect on larger samples [14].

In this blockade regime, an effective two-level system is realized between the state with all atoms in the ground level and

the single-excitation symmetric atomic state. This two-level system has an effective light-atom coupling that is a factor of \sqrt{N} larger than the light-single-atom coupling. It is promising for a wide variety of quantum information processing applications [20–26]. In the following two subsections, we briefly review the collective encoding strategy for a k -bit quantum register [23] and the cooperative photon emission effect [25–28] in a Rydberg blockade coupled ensemble, which are directly related to our repeater scheme.

A. Collective encoding in a Rydberg blockade coupled ensemble

A Rydberg coupled atomic ensemble consisting of N atoms can be used to build a k -bit quantum register ($N \gg k$), where the qubits are collectively encoded in different single excitation symmetric atomic states [23]. As shown in Fig.1(a), k qubits are encoded in an ensemble of N atoms with $2k + 1$ long-lived ground levels. The i -th qubit values zero and one are identified with symmetric single-excitation atomic states populating $|0_i\rangle$ and $|1_i\rangle$, respectively. The initialization of this k -bit register is as follows: Originally all the atoms are in the reservoir state $|g\rangle$. Then due to the blockade mechanism, one can transfer precisely one atom to each pair of levels ($|0_i\rangle, |1_i\rangle$) via a Raman transition involving a Rydberg state $|r\rangle$.

In the following, for given atomic levels $|x_i\rangle (x = 0, 1, i = 1 \dots k)$, we will let the kets $|\tilde{x}_i\rangle (x = 0, 1, i = 1 \dots k)$ denote the symmetric single-excitation collective atomic states, for instance,

$$|\tilde{1}_1\rangle = \frac{1}{\sqrt{N}} \sum_{j=1}^N e^{-i\vec{k}_0 \cdot \vec{r}_j} |g\rangle_1 |g\rangle_2 \dots |1_1\rangle_j \dots |g\rangle_N, \quad (1)$$

where \vec{r}_j is the position of the j -th atom, $|1_1\rangle_j$ indicates that the j -th atom is in the state $|1_1\rangle$, and \vec{k}_0 is the summation of all the wave vectors of the light pulses used to transfer the ensemble to the above state, i.e., $\vec{k}_0 = \sum_m \lambda_m \vec{k}_m$, and $\lambda_m = \pm 1$, depending on whether a photon is absorbed or emitted during the m -th pulse. Accordingly, the basis of the i -th qubit can be written as ($|\tilde{0}_i\rangle, |\tilde{1}_i\rangle$).

It has been proposed in Ref. [23] that both single-bit rotations and two-qubit gates can be realized in this system. The single-qubit rotations on the i -th qubit are straightforwardly performed using two-photon stimulated Raman beams coupling $|0_i\rangle$ and $|1_i\rangle$. The two-qubit phase gate between the j -th and k -th qubits is implemented by a sequence of three laser pulses as shown in fig.1(b): (i) The excitation of the control qubit internal state $|0_j\rangle$ into one Rydberg state $|r_1\rangle$; (ii) 2π Rabi rotation between the target qubit state $|0_k\rangle$ and another Rydberg state $|r_2\rangle$; (iii) The return of the population from $|r_1\rangle$ to $|0_j\rangle$. If the control qubit is in state $|0\rangle$, the resulting unit occupancy of the $|r_1\rangle$ state blocks the Rabi cycle and nothing happens to the target qubit, while a control qubit in state $|1\rangle$ causes no blockade, and hence we obtain a controlled π phase shift on the $|0_k\rangle$ state amplitude due to a full Rabi cycle. Hence, universal quantum computing operations can be realized in this system [23].

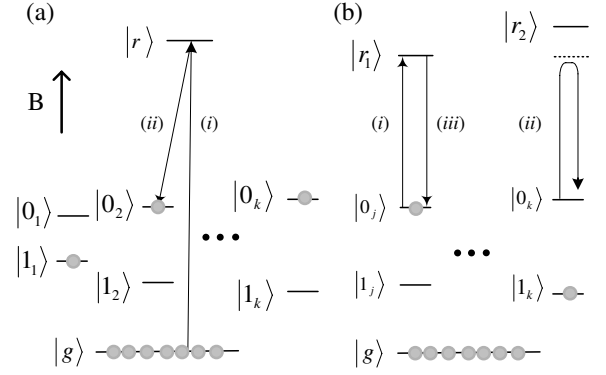


FIG. 1: (a) Collective encoding of k qubits in an ensemble of N atoms (gray dots) with $2k + 1$ long-lived levels; $|r\rangle$ is a Rydberg state, and $|x_i\rangle (x = 0, 1, i = 1 \dots k)$ and $|g\rangle$ are ground states. A magnetic field B is applied to the ensemble, which enables every ground state to be selectively manipulated via appropriate choices of laser frequencies. The transitions (i) and (ii) show the initialization procedure of the second qubit. (b) Two-qubit phase gate on collectively encoded qubits j and k mediated by Rydberg blockade. See text for details.

B. Cooperative photon emission from a Rydberg blockade coupled ensemble

Now we discuss how to map a collectively encoded qubit in the ensemble into a flying photonic qubits. Assume the ensemble is in the state $|\tilde{1}_f\rangle$. If one transfers state $|\tilde{1}_f\rangle$ into an excited state $|\tilde{e}\rangle$ via a π -pulse laser with wave vector \vec{k}_e , this state will radiate into a variety of modes with all the atoms in state $|g\rangle$ and a single-photon propagating with the wave vector \vec{k} . The amplitude for emitting a photon with wave vector \vec{k} and polarization \vec{e} , is proportional to

$$\langle g_1 \dots g_N | \langle \vec{k} | (\vec{e} \cdot \vec{d}) \hat{a}_k^\dagger | \tilde{e} \rangle | \text{vac} \rangle = - \sum_{j=1}^N \frac{\langle g | (\vec{e} \cdot \vec{d}) | e \rangle e^{-i(\vec{k}_0 + \vec{k}_e - \vec{k}) \cdot \vec{r}_j}}{\sqrt{N}}, \quad (2)$$

where \hat{a}_k^\dagger is the creative operator for a photon in mode \vec{k} and \vec{d} is the dipole operator. Thus the transition probability $P(\vec{k})$ is proportional to

$$P(\vec{k}) \propto \frac{1}{N} \left| \sum_{j=1}^N e^{-i(\vec{k}_0 + \vec{k}_e - \vec{k}) \cdot \vec{r}_j} \right|^2. \quad (3)$$

Note that if $\vec{k}_0 + \vec{k}_e = \vec{k}$ all the phase terms are zero and $P(\vec{k}) \propto N$; otherwise the phase terms become random so that $P(\vec{k}) \propto 1$, which means the emission is highly directional. Although the typical size of a Rydberg blockade coupled ensemble is less than $10\mu\text{m}$ consisting of only several hundreds of atoms [14], the above cooperative emission effect is still large enough to ensure very good directed emissions of photons [25–28], cf. below.

There are two different ways to convert a collectively encoded qubit $\alpha|\tilde{0}_f\rangle + \beta|\tilde{1}_f\rangle$ into a flying photonic polarization qubit $\alpha|h\rangle + \beta|v\rangle$, where h and v indicate the horizontal and

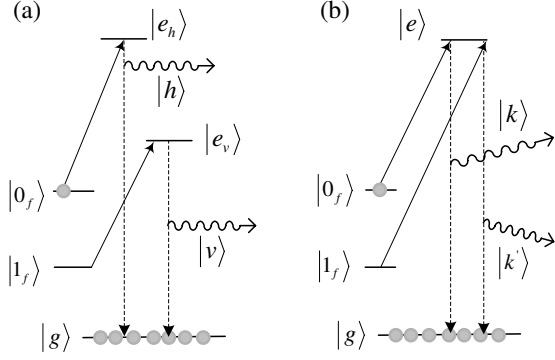


FIG. 2: Two different ways to convert a collectively encoded qubit into a photonic qubit, cf.text.

vertical polarization, respectively. On the one hand, using polarization selection rules, one can transfer the state $|\tilde{0}_f\rangle$ and $|\tilde{1}_f\rangle$ to excited states $|\tilde{e}_h\rangle$ and $|\tilde{e}_v\rangle$, respectively, and the subsequent atomic decay to the state $|g_1 \cdots g_N\rangle$ leads to emission of the photonic state (Fig.2(a)). However, the horizontal and vertical amplitudes may have different frequencies. While this does not prevent the creation of entanglement between remote ensembles, it makes it more challenging to prove intermediate ensemble-photon entanglement experimentally. On the other hand, one can use only one excited state $|e\rangle$ and appropriately choose the wavevectors of the lasers for transitions ($\vec{k}_e : |\tilde{0}_f\rangle \rightarrow |\tilde{e}\rangle$) and ($\vec{k}'_e : |\tilde{1}_f\rangle \rightarrow |\tilde{e}\rangle$). Thus the cooperative emission from $|\tilde{e}\rangle$ to $|g_1 \cdots g_N\rangle$ is directed into different directions \vec{k} and \vec{k}' due to the phase matching condition, as shown in Fig.2(b). Then the photonic state $\alpha|\vec{k}\rangle + \beta|\vec{k}'\rangle$ can be easily changed into photonic polarization state $\alpha|h\rangle + \beta|v\rangle$ by linear optics.

III. REPEATER BASED ON RYDBERG BLOCKADE COUPLED ENSEMBLES

A. Main idea and efficiency

In our scheme, each repeater node contains a single ensemble collectively encoding three qubits. As shown in Fig.3, qubit s ($s=1,2$) is a stationary qubit, and qubit f is responsible for producing a flying photonic qubit. To establish entanglement between ensemble A and ensemble B , we first focus on qubit 1 and qubit f in these two ensembles. In each ensemble, we prepare the entangled state $(|\tilde{0}_1\rangle|\tilde{0}_f\rangle + |\tilde{1}_1\rangle|\tilde{1}_f\rangle)/\sqrt{2}$ using the single-bit and two-qubit gate described in the previous section. Then qubit f in each ensemble is converted into a photonic polarization state via the method shown in fig.2. The joint state of the two emitted photons and of ensembles A and B can be expressed as

$$|\psi^A\rangle \otimes |\psi^B\rangle = (|\tilde{0}_1\rangle_A|h\rangle_A + |\tilde{1}_1\rangle_A|v\rangle_A) \otimes (|\tilde{0}_1\rangle_B|h\rangle_B + |\tilde{1}_1\rangle_B|v\rangle_B)/2. \quad (4)$$

Combining the two emitted photons on a polarizing beam

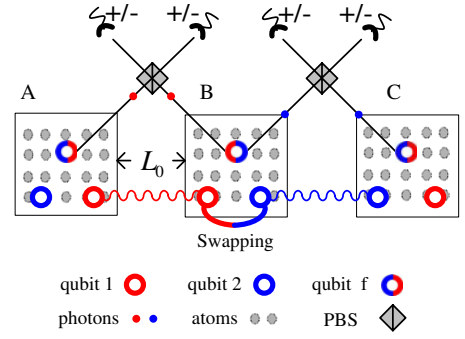


FIG. 3: (Color online) Quantum repeater based on Rydberg blockade coupled ensembles. Neighboring nodes are separated by a distance L_0 . Each node consists of one atomic ensemble encoding three qubits, qubit 1 (red circle), qubit 2 (blue circle) and qubit f (two-tone circle). Each ensemble asynchronously emits two single photons (red and blue dots), which are entangled with qubits 1 and 2 (red and blue circles), respectively. Then the photons will be measured in the middle stations by polarizing beam splitters (PBSs) and photon detectors. When certain two-photon coincidences are observed, the 'red' ('blue') qubits in neighboring ensembles are projected into entangled states. Then entanglement is extended to long distances by entanglement swapping operations via two-qubit gates on qubits 1 and 2 in the same ensemble.

splitter (PBS) at a central station located half-way between ensembles A and B , a probabilistic Bell state analysis can be performed by counting the photon number in each output mode $d_{\pm} = \frac{1}{\sqrt{2}}(|h\rangle_A \pm |v\rangle_B)$ and $\tilde{d}_{\pm} = \frac{1}{\sqrt{2}}(|h\rangle_B \pm |v\rangle_A)$. Such Bell analysis projects non-destructively the two ensembles into an entangled state. In particular, the detection of two photons, one in each mode d_+ and \tilde{d}_+ , leads to the entangled state

$$|\psi^{AB}\rangle = (|\tilde{0}_1\rangle_A|\tilde{0}_1\rangle_B + |\tilde{1}_1\rangle_A|\tilde{1}_1\rangle_B)/\sqrt{2}. \quad (5)$$

In the ideal case, the probability for such an event is $1/8$. Taking into account the coincidences between $d_+ - \tilde{d}_-$, $d_- - \tilde{d}_+$ and $d_- - \tilde{d}_-$ combined with the appropriate one-qubit operations, the probability to get the state (5) is $1/2$ (in the absence of transmission losses etc., cf. below).

In this manner, the entanglement can be established between ensembles $A - B$, $C - D$, etc. To entangle the remaining links, the procedure will be repeated with qubit 2 and qubit f between ensembles $B - C$, $D - E$, etc. Considering two links, say $A - B$ and $B - C$, the resulting state after successful entanglement creation is

$$|\psi^{AB}\rangle \otimes |\psi^{BC}\rangle = (|\tilde{0}_1\rangle_A|\tilde{0}_1\rangle_B + |\tilde{1}_1\rangle_A|\tilde{1}_1\rangle_B)(|\tilde{0}_2\rangle_B|\tilde{0}_2\rangle_C + |\tilde{1}_2\rangle_B|\tilde{1}_2\rangle_C)/2. \quad (6)$$

We now calculate the time needed for entanglement creation between two neighboring ensembles, which are separated by a distance L_0 . Let us denote by p the success probability for an ensemble to emit a photon, including the probability to prepare the entangled state between qubit s and qubit f , the efficiency of converting qubit f into a photon

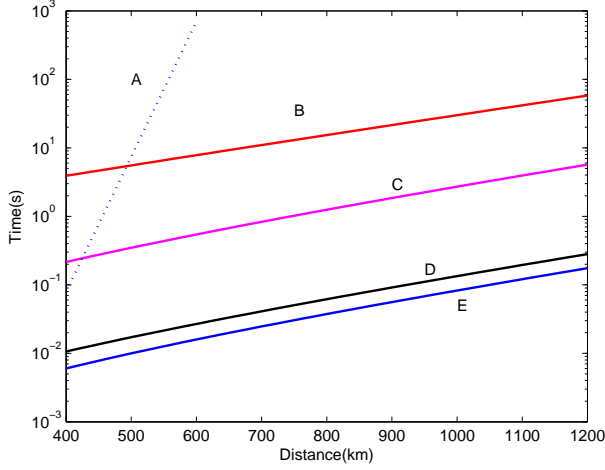


FIG. 4: (Color online) Performance of quantum repeaters based on Rydberg blockade coupled ensembles. The quantity shown is the average time needed to distribute a single entangled pair for the given distance. We assume losses of 0.2 dB/km, corresponding to telecom fibers at a wavelength of 1.5 μm . Curve A: as a reference, the time required using direct transmission of photons through optical fibers with a single-photon generation rate of 10 GHz. Curve B: the most efficient DLCZ-type repeater scheme known to us [8]. In this scheme high-fidelity entangled pairs are generated locally, and entanglement generation and swapping operations are based on two-photon detections. We have assumed memory and detector efficiencies of 0.9. Curves C and D: schemes based on Rydberg blockade coupled ensembles with $p = 0.2$ and $p = 0.9$, respectively. Curve E: scheme based on trapped ions in high-finesse cavities, where the success probability for the ion to emit a photon is 0.9. Notice that we imposed a maximum number of 16 links in the repeater chain for curves B, C, D and E.

and coupling it into the fiber. The probability to get the expected twofold coincidence is thus given by $P_0 = \frac{1}{2}p^2\eta_d^2\eta_t^2$, where η_d is the photon detection efficiency and $\eta_t = \exp\left(-\frac{L_0}{2L_{att}}\right)$ is the transmission efficiency corresponding to a distance of $\frac{L_0}{2}$, where L_{att} is the fiber attenuation length. Here we assume the losses in the fiber are 0.2dB/km, corresponding to $L_{att} = 22\text{km}$. The entanglement creation attempts can be repeated at time $t_p + t_{com}$, where $t_{com} = L_0/c$ is the communication time and $c = 2 \times 10^8\text{m/s}$ is the light velocity in the fiber [15]. We assume a typical preparation $t_p = 20\mu\text{s}$, cf. below. As a consequence, the average time required to entangle two ensembles separated by a distance L_0 is given by

$$T_{link} = \frac{t_p + t_{com}}{P_0} = \frac{2(t_p + L_0/c)}{p^2\eta_d^2\eta_t^2}. \quad (7)$$

The entanglement can further be distributed over longer distances by using successive entanglement swapping operations between elementary links. Such swapping operations require a local Bell state analysis, applied, for example, on the qubit 1 and qubit 2 in ensemble B to entangle ensembles A and C . Thanks to the high-fidelity single-bit and two-qubit gates available in our system, the success probability of entanglement swapping is only restrained by the read-out efficiency.

An effective read-out mechanism in this context can be realized by state-selective ionization [29]. By coupling different ground levels to different excited states and selectively ionizing them, the resulting electron and ion can be detected by channel electron multipliers. As it is sufficient to detect at least one of the ionization fragments, the overall detection efficiency can be as high as $\eta_{ion} = 95\%$ [29]. Hence, the success probability of entanglement swapping is $P_{swap} = 1/\eta_{ion}^2$, and the total time for the distribution of an entangled pair over the distance $2L_0$ is given by

$$T_{2L_0} = \frac{3}{2} \left(t_p + \frac{L_0}{c}\right) \frac{1}{P_0 P_{swap}} = 3 \left(t_p + \frac{L_0}{c}\right) \frac{1}{p^2\eta_t^2\eta_d^2\eta_{ion}^2}. \quad (8)$$

The factor 3/2 takes into account the fact that for the swapping attempt one has to establish two neighboring links. If the average waiting time for entanglement generation for one link is T , there will be a success for one of the two after $T/2$; then one still has to wait a time T on average for the second one, giving a total of $3T/2$. This simple argument gives exactly the correct result in the limit of small P_0 . In a repeater with n nesting levels, the precise values of analogous factors have no analytic expression, but numerical results show that this remains a good approximation [30]. Hence, the total time required for a successful entanglement distribution over the distance $L = 2^n L_0$ can be expressed as

$$\begin{aligned} T_{tot} &\approx \left(\frac{3}{2P_{swap}}\right)^n \left(t_p + \frac{L_0}{c}\right) \frac{1}{P_0} \\ &= \left(t_p + \frac{L_0}{c}\right) \frac{3^n}{2^{n-1} p^2 \eta_d^2 \eta_t^2 \eta_{ion}^{2n}}. \end{aligned} \quad (9)$$

We calculate the performance of a quantum repeater based on Rydberg blockade coupled ensembles with Eq.(9), as shown in Fig. 4. In the same figure we also show the performance of the most efficient DLCZ-type repeater known to us [8], and that of a repeater based on trapped ions [13]. One can see that the achievable performance for repeaters based on Rydberg blockade coupled ensembles greatly exceeds the best DLCZ-type repeater, and is comparable with the repeater based on trapped ions with high-finesse cavities. Another feature of repeaters based on Rydberg blockade coupled ensembles is that the average time for the distribution of an entangled pair scales only like $1/p^2$, in contrast to the DLCZ-type repeaters which are much more sensitive to a reduction in memory efficiencies. As can be seen from Fig.4, even with $p = 0.2$, the entanglement distribution time of our scheme is still 10 times shorter than the time achievable with the best known DLCZ-type repeater protocol.

B. Implementation and noise analysis

In this paper, we focus on realizing the present scheme with ^{87}Rb , whose nuclear spin $I = 3/2$ provides 8 stable Zeeman states in the $f=1,2$ hyperfine levels (Fig.5). A modest magnetic field of $B \sim 20\text{G}$ is applied to the atoms, which gives splitting among the above Zeeman states at least $\delta_E = \frac{\mu_B B}{2\hbar} \sim 14\text{MHz}$,

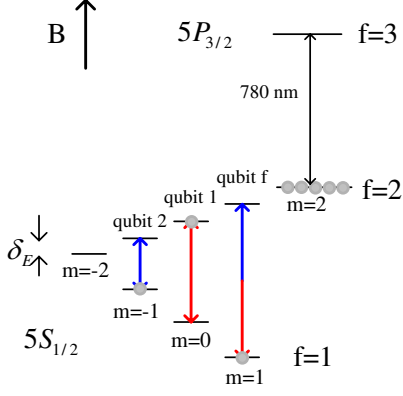


FIG. 5: (Color online) ^{87}Rb level scheme and identification of a three-qubit quantum register. See text for details.

where μ_B is the Bohr magneton. Initially, all the atoms are in the reservoir state $|5S_{1/2}, f=2, m=2\rangle$. Qubit s ($s=1,2$) and qubit f are encoded in other six Zeeman states via collective encoding, as shown in Fig.5. The state $|5P_{3/2}, f=3, m=2\rangle$ is employed as $|e\rangle$ for mapping qubit f into photonic qubits so that the wavelength of the emitted photons is $\lambda = 780\text{nm}$.

In principle, any atomic ensembles that are suitable for collective encoding strategy can be used to implement the present scheme [23]. To be specific, we first study a cubic lattice with several hundreds of atoms. It should be noted that our scheme has a significant flexibility of the shape and density of the ensemble, cf. below. For now let us suppose that an ordered three-dimensional array of $7 \times 7 \times 15 = 735$ ^{87}Rb atoms is loaded into an elongated optical lattice. With a lattice spacing of $0.37\mu\text{m}$, the maximum distance between any two atoms is $R_{\text{max}} \approx 6\mu\text{m}$. We carefully choose two Rydberg states $|r_1\rangle$ and $|r_2\rangle$, ensuring that the usual C_5/R^5 or C_6/R^6 van-der-Waals interaction is resonantly enhanced by Föster processes leading to isotropic C_3/R^3 long-range interaction [19, 22, 23]. Assuming the principal quantum number of the Rydberg states is $n = 80$, a blockade shift as large as $\mathbf{B}/2\pi \geq 10\text{MHz}$ at a separation of $6\mu\text{m}$ is achievable [19, 23].

Based on the above specific physical system, we now analyze the error sources and determine the optimal Rabi frequencies for transitions in our scheme. The main errors in our scheme arise in the procedures involving Rydberg blockade, including the initializations of qubit s ($s=1,2$) and qubit f , two-qubit phase gate for creating entanglement between qubit s and qubit f , and two-qubit phase gate for entanglement swapping. One can estimate the errors by adding the contributions from the physically distinct processes of spontaneous emission from Rydberg states and imperfect blockade errors, which are due to the double excitation of Rydberg states. Using the techniques developed in [31], we calculate the double excitation probability P_2 and spontaneous emission probability P_{loss} for the above four different procedures (as shown in Table I).

It should be noted that in our system the cooperative spontaneous emission dominates the decay processes from Ryd-

berg states. Thus the atoms in the Rydberg states are most likely to decay to the reservoir state (with a probability of order $d/(d+1)$, where d is the optical depth of the ensemble). If so, after spontaneous emission the state of the ensemble will be outside the subspace spanned by qubit s and qubit f , and thereby can be eliminated by the following post-selection measurement of our repeater scheme. Hence, all the spontaneous emission error terms are suppressed by a factor $1/(d+1)$. The double excitation in the procedure of initializing qubit s results in two ions in the selective ionization measurement in the swapping, and thus induces an error with a probability of $2(1 - \eta_{\text{ion}})\eta_{\text{ion}}P_2^{(is)} \approx 0.1P_2^{(is)}$. A double excitation in the procedure of initializing qubit f leads to a two-photon emission into the fiber, which gives an error as large as $2P_2^{(if)}$. Double excitations which occur in the two-qubit gates for entanglement creation or entanglement swapping will cause the final state to be separable. They introduce errors with probabilities of $P_2^{(en)}$ and $P_2^{(sw)}$, respectively. For clarity, we show all the errors corresponding to the different procedures in Table I. The error in the entanglement creation $E^{(c)}$ can be written as

$$\begin{aligned} E^{(c)} &= E^{(is)} + E^{(if)} + E^{(en)} \\ &= \frac{0.1\Omega_s^2}{2\mathbf{B}^2} + \frac{3\pi}{2\tau\Omega_s(d+1)} + \frac{9\Omega_f^2}{8\mathbf{B}^2} + \frac{9\pi}{4\tau\Omega_f(d+1)}. \end{aligned} \quad (10)$$

All the above errors result in a separable component ρ_{sep} in the created state with the probability $E^{(c)}$, where the specific form of ρ_{sep} is not important to our discussion. Hence, the density matrix of each link after the entanglement creation reads

$$\rho_0 \approx |\psi\rangle\langle\psi| + E^{(c)}\rho_{\text{sep}}, \quad (11)$$

where $|\psi\rangle$ is the desired entangled state and ρ_{sep} is the error term. The error term will be amplified by subsequent swapping operations. Taking into account the error in the entanglement swapping $E^{(sw)}$, after the n -th swapping operation the density matrix of final state is

$$\rho_n \approx |\psi\rangle\langle\psi| + [2^n E^{(c)} + (2^n - 1)E^{(sw)}]\rho_{\text{sep}}. \quad (12)$$

Note that for ultra-cold atoms trapped in an optical lattice, the lifetime of a Rydberg state with $n = 80$ is about $500\mu\text{s}$. The optical depth $d = N\lambda^2/A$ in such a $7 \times 7 \times 15$ optical lattice is around 10, where A is the cross section of the ensemble. Assuming a nesting level $n = 4$ (corresponding to $2^4 = 16$ links), one can straightforwardly derive the optimal Rabi frequencies $\Omega_{f\text{opt}}/2\pi = 0.415\text{MHz}$ and $\Omega_{s\text{opt}}/2\pi = 0.209\text{MHz}$, which minimize the error term in Eq.(12), resulting in the fidelity of the final entangled state $F \approx 0.977$.

Now we use the parameters described above to estimate p , i.e., the success probability for an ensemble to emit a photon. Suppose one can collect the photon emitted in a direction within 0.3 rad off the axis of the ensemble as in Ref. [32]. Based on Eq.(3), we can predict that the photon is emitted into the collectable area with more than 93% probability. Taking spontaneous emission in the preparation of ensemble-photon entanglement state into account, we estimate $p \approx 0.9$. The performance of a repeater with the above configuration is shown as curve D in Fig.4.

Note that our scheme is quite robust to a reduction of p , resulting in a significant flexibility of the requirements for the atomic ensemble. For example, instead of the optical lattice, we could use an atomic sample where 200 atoms are randomly positioned within a $6\mu\text{m}$ diameter sphere, resulting in a moderate optical depth $d \approx 1$. Using the same method as above, we can derive that now $p \approx 0.2$ with the maximum fidelity of the final entangled state $F \approx 0.927$. As shown by curve C in Fig.4, the performance of our scheme with this configuration still outperforms the DLCZ-type repeater by at least one order of magnitude.

C. Additional speed-up via temporal multiplexing

As seen in the previous subsections, the creation of entanglement between neighboring nodes A and B is heralded on the outcome of photon detections at a middle station. To benefit from a nested repeater, the entanglement swapping operations can only be performed once one knows the relevant measurement outcomes. This requires a communication time of order L_0/c . If every node consists of a multiqubit register, and the entanglement creation in the register can be triggered m times in every communication time interval L_0/c , one can decrease the average time for entanglement creation T_{link} by a factor of order m [15]. We here propose a realization of the same basic idea for quantum repeaters based on Rydberg blockade coupled ensembles.

As said before, the collective encoding strategy provides a promising way to realize a multiqubit register. For instance, Ref. [33] proposed to use a single holmium ensemble to realize a 60-qubit register via collective encoding. Note that in such a 60-qubit register every qubit can be separately addressed and two-qubit gates between any two qubits are achievable [33]. Suppose we use such a 60-qubit register as the quantum memory in each node. Take ensemble B as an example, one of the 60 qubits in ensemble B is used to emit single photons, and other 58 qubits are equally divided into two groups (“red” and “blue”) as stationary qubits. Using the same procedure shown in Fig.2, the qubits in the “red” and

“blue” groups are alternately entangled with corresponding emitted single photons, which are sent toward ensembles A or C, respectively. If there are two detections in the central station located between A and B for the k -th qubit for example, then we know that these qubits are entangled. Running the same scheme for the qubits in the other group, there may be similar detections between B and C locations associated to the l -th qubits. One then performs the Bell state analysis for entanglement swapping by applying a two-qubit gate on the k -th and l -th qubits, thus creating entanglement between ensembles A and C. Using such a holmium ensemble register could increase the entanglement distribution rate of the studied scheme by up to a factor of 29.

IV. CONCLUSION

We have shown that Rydberg blockade coupled ensembles are very promising systems for the implementation of quantum repeaters. Compared with DLCZ-type repeaters, our scheme improves the entanglement distribution rate by several orders of magnitude. One reason is that for Rydberg blockade coupled atomic ensembles the entanglement swapping operations are performed almost deterministically, in contrast to success probabilities below 0.5 per swapping for DLCZ-type repeaters. Another reason is that the blockade mechanism suppresses multiple emissions from individual ensembles so that our scheme does not need to work with a very low emission probability. Compared with repeaters based on trapped ions, both the entanglement fidelity and the distribution rate of our scheme are comparable. This is because a Rydberg blockade coupled atomic ensemble behaves as one superatom with a two-level structure. However, by using an ensemble based scheme we avoid the requirements of a high-finesse cavity, and of addressing and transporting single ions. Moreover, our scheme is amenable to temporal multiplexing, which could further improve the performance.

Acknowledgments. We thank A. Lvovsky and A. MacRae for useful discussions.

Note added. After completion of this work we became aware of a very recent similar proposal [34].

-
- [1] C. H. Bennett, G. Brassard, C. Crépeau, R. Jozsa, A. Peres, and W. K. Wootters, Phys. Rev. Lett. **70**, 1895 (1993).
 - [2] A. K. Ekert, Phys. Rev. Lett. **67**, 661 (1991).
 - [3] H.-J. Briegel, W. Dür, J.I. Cirac, and P. Zoller, Phys. Rev. Lett. **81**, 5932 (1998).
 - [4] L.-M. Duan, M.D. Lukin, J.I. Cirac, and P. Zoller, Nature **414**, 413 (2001).
 - [5] L. Jiang, J.M. Taylor, and M.D. Lukin, Phys. Rev. A **76**, 012301 (2007).
 - [6] Z.-B. Chen *et al.*, Phys. Rev. A **76**, 022329 (2007); B. Zhao *et al.*, Phys. Rev. Lett. **98**, 240502 (2007).
 - [7] N. Sangouard *et al.*, Phys. Rev. A **76**, 050301(R) (2007).
 - [8] N. Sangouard *et al.*, Phys. Rev. A **77**, 062301 (2008).
 - [9] C.-W. Chou *et al.*, Science **316**, 1316(2007); Z.-S. Yuan *et al.*, Nature **454**, 1098 (2008).
 - [10] J. Calsamiglia and N. Lütkenhaus, Appl. Phys. B **72**, 67 (2001).
 - [11] B. He *et al.*, Phys. Rev. A **79**, 052323 (2009); M. S. Shahriar, G. S. Pati, and K. Salit, Phys. Rev. A **75**, 022323 (2007).
 - [12] L. Childress *et al.*, Phys. Rev. Lett. **96**, 070504 (2006); C. Simon *et al.*, Phys. Rev. B **75**, 081302(R) (2007); P. Van Loock, N. Lütkenhaus, W.J. Munro, and K. Nemoto, Phys. Rev. A **78**, 062319 (2008).
 - [13] N. Sangouard, R. Dubessy, and C. Simon Phys. Rev. A **79**, 042340 (2009)
 - [14] M. Saffman, T. G. Walker, and K. Mølmer, arXiv:0909.4777.
 - [15] C. Simon *et al.*, Phys. Rev. Lett. **98**, 190503 (2007).
 - [16] T. F. Gallagher, *Rydberg Atoms* (Cambridge University Press, Cambridge, 1994).
 - [17] D. Jaksch *et al.*, Phys. Rev. Lett. **85**, 2208 (2000).
 - [18] A. Gaëtan *et al.*, Nature Phys. **5**, 115 (2009). E. Urban *et al.*, Nature Phys. **5**, 110 (2009).
 - [19] L. Isenhower *et al.*, Phys. Rev. Lett. **104**, 010503 (2010); T.

- Wilk *et al.*, Phys. Rev. Lett. **104**, 010502 (2010).
- [20] M. D. Lukin *et al.*, Phys. Rev. Lett. **87**, 037901 (2001).
- [21] M. Saffman and T. G. Walker, Phys. Rev. A **72**, 042302 (2005).
- [22] M. Saffman and T. G. Walker, Phys. Rev. A **72**, 022347 (2005); T. G. Walker and M. Saffman, J. Phys. B **38**, S309 (2005).
- [23] E. Brion, K. Mølmer, and M. Saffman, Phys. Rev. Lett. **99**, 260501 (2007).
- [24] M. Müller *et al.*, Phys. Rev. Lett. **102**, 170502 (2009); M. Saffman and K. Mølmer, Phys. Rev. Lett. **102**, 240502 (2009).
- [25] M. Saffman and T. G. Walker, Phys. Rev. A **66**, 065403 (2002).
- [26] L. H. Pedersen and K. Mølmer, Phys. Rev. A **79**, 012320 (2009).
- [27] A. E. B. Nielsen and K. Mølmer, arXiv:1001.1429.
- [28] D. Porras and J. I. Cirac, Phys. Rev. A **78**, 053816 (2008).
- [29] W. Rosenfeld *et al.*, Adv. Sci. Lett. **2**, 469 (2009).
- [30] O.A. Collins, S.D. Jenkins, A. Kuzmich, and T.A.B. Kennedy, Phys. Rev. Lett. **98**, 060502 (2007); J.B. Brask and A.S. Sørensen, Phys. Rev. A **78**, 012350 (2008).
- [31] M. Saffman and T. G. Walker, Phys. Rev. A **72**, 022347 (2005).
- [32] S. Yoon *et al.*, J. Phys.: Conf. Ser. **80**, 012046 (2007).
- [33] M. Saffman and K. Mølmer, Phys. Rev. A **78**, 012336 (2008).
- [34] B. Zhao, M. Müller, K. Hammerer, and P. Zoller, arXiv:1003.1911.

TABLE I: The double excitation probability P_2 , spontaneous emission probability P_{loss} and relevant errors in four different procedures involving Rydberg blockade in our scheme. We denote the Rabi frequencies corresponding to qubit s and qubit f by Ω_s and Ω_f , respectively; τ is the lifetime of Rydberg state and d is the optical depth of the ensemble. Since qubit s and qubit f play different roles in different procedures, the errors caused by P_2 and P_{loss} need to be calculated separately for each. See text for details.

Procedures involving Rydberg blockade	P_2	P_{loss}	Error caused by P_2 and P_{loss}
Initializing qubit s	$P_2^{(is)} = \Omega_s^2/2\mathbf{B}^2$	$P_{loss}^{(is)} = \pi/\tau\Omega_s$	$E^{(is)} = 2(1 - \eta_{ion})\eta_{ion}P_2^{(is)} + P_{loss}^{(is)}/(d + 1)$
Initializing qubit f	$P_2^{(if)} = \Omega_f^2/2\mathbf{B}^2$	$P_{loss}^{(if)} = \pi/\tau\Omega_f$	$E^{(if)} = 2P_2^{(if)} + P_{loss}^{(if)}/(d + 1)$
Entangling qubit s and qubit f	$P_2^{(en)} = \Omega_f^2/8\mathbf{B}^2$	$P_{loss}^{(en)} = 5\pi/4\tau\Omega_f + \pi/2\tau\Omega_s$	$E^{(en)} = P_2^{(en)} + P_{loss}^{(en)}/(d + 1)$
Swapping	$P_2^{(sw)} = \Omega_s^2/8\mathbf{B}^2$	$P_{loss}^{(sw)} = 7\pi/4\tau\Omega_s$	$E^{(sw)} = P_2^{(sw)} + P_{loss}^{(sw)}/(d + 1)$